4E3-3

Eigenmodes Analysis in Drude-Type Dispersive EBG Structures in Frequency Domain

[#]Amin Gul HANIF [1], Takuji ARIMA[2] , and Toru UNO [3]

[1] 50012894005@st.tuat.ac.jp , [2] t-arimia@cc.tuat.ac.jp, [3] uno@cc.tuat.ac.jp,

Electronic and Information Engineering Department, Graduate School of
Engineering, Tokyo University of Agriculture and Technology
2-24-16 Naka-cho, Koganei-shi, Tokyo, Japan 184-0012

1. Introduction

Recently, remarkable progress has been made in the study of electromagnetic band gap (EBG) structures due to their various applications in optics, microwave, and antenna engineering [1]. The band structure of EBG structures has been researched for frequency-independent or non-dispersive materials. Lately, there is an intensive interest in the analysis of dispersive EBG structures for novel applications. Therefore, accuracy in modeling of the band structure of EBGs composed of dispersive materials is important to accurately analyze the wave propagation phenomena over a wide range of frequencies in microwave and optical fields.

Several numerical methods have been used for the band structure computation of two-dimensional (2D) EBG structures. The most commonly used methods are the plane-wave expansion (PWE) method [2], the finite-difference time-domain (FDTD) method [3-5], and the finite-difference frequency-domain (FDFD) method [1, 6]. The PWE method is very simple and easy to apply. However, the resultant matrix of the PWE method is dense and large, therefore making its computation heavy for large problems. The FDTD method is a widely-used electromagnetic computational method, which is also applicable for dispersive materials [5]. However, in some cases, the FDTD method does not give accurate results for the band structure calculation of EBG media because there is a chance of losing the resonant frequencies if the excitation and monitor points are not properly located in the calculation domain [3, 6]. In addition, the FDTD has limitations in resolving the degenerate eigenmodes [3].

On the other hand, the FDFD method is highly accurate in band structure computation of EBG structures [1, 6]. Because FDFD relies on linear algebra and uses the eigenvalue equation to calculate the eigenvalue of the characteristic matrix, and it is capable to calculate the eigenfrequencies clearly even if they are very close to each other or degenerate. Nevertheless, it has not been possible to calculate the band structure of dispersive materials with the FDFD method. Lately, the authors developed improved 2-D FDFD algorithm [7] that can calculate the band structure and field distribution of Debye-type dispersive EBG media.

In this paper, we use a new 2D FDFD algorithm to calculate the band structure and electric field distribution of eigenmodes of 2D EBG structure composed of Drude-type dispersive media. This algorithm uses only the eigenvalue equation, thus, all of the eigenfrequencies can be computed accurately for every band point of irreducible Brillouin zone. To validate this method, it is compared with the FDTD method which shows high accuracy and stability.

2. Formulation

The formulation has been developed for TM_z mode, single-pole Drude-type dispersive materials. For, TM_z mode the Maxwell's equations can be written in the matrix equation form as

$$j\omega \begin{bmatrix} \varepsilon_0 \varepsilon_z^{'} & 0 & 0 \\ 0 & -\mu_0 \mu_x & 0 \\ 0 & 0 & -\mu_0 \mu_y \end{bmatrix} \begin{bmatrix} E_z \\ H_x \\ H_y \end{bmatrix} = \begin{bmatrix} 0 & -V_y & V_x \\ U_y & 0 & 0 \\ -U_x & 0 & 0 \end{bmatrix} \begin{bmatrix} E_z \\ H_x \\ H_y \end{bmatrix} \tag{1}$$

where $\varepsilon_z^{'}$ is a diagonal matrix composed of Drude relative permittivity at the grid points; $\mathbf{V_x}, \mathbf{V_y}, \mathbf{U_x}$, and $\mathbf{U_y}$ are square matrices containing space-differential operators along x and y directions; $\mathbf{\mu}_x$ and $\mathbf{\mu}_y$ are diagonal matrices of relative permeability at the grid points; $\mathbf{H_x}, \mathbf{H_y}$, and $\mathbf{E_z}$ are column matrices containing the field values. Periodic boundary conditions, on the square unit cell as shown in Fig. 1(a), are placed in the space-differential operators [1]. For simplicity, we eliminate $\mathbf{H_x}$ and $\mathbf{H_y}$ from (1), which leads to

$$-\omega^2 \varepsilon_0 \varepsilon_z^{'} \mathbf{E}_z - \mathbf{A}\,\mathbf{E}_z = 0 \tag{2}$$

Where $\mathbf{A}$ is a sparse matrix composed of space differential operators and the inverse of relative permeability matrices

$$\mathbf{A} = \frac{1}{\mu_0}(\mathbf{V_y} * \mathbf{\mu_x}^{-1} * \mathbf{U_y} + \mathbf{V_x} * \mathbf{\mu_y}^{-1} * \mathbf{U_x}) \tag{3}$$

we use the Drude relative permttivity $\varepsilon_r(\omega) = 1 + \dfrac{\omega_p^2}{-\omega^2 + j\omega v_c}$ into (2) and can write

$$-\omega^2 \varepsilon_0 \left(\mathbf{I} + \frac{\omega_p^2}{-\omega^2 \mathbf{I} + j\omega \mathbf{v}_c} \right) \mathbf{E}_z = \mathbf{A}\mathbf{E}_z \tag{4}$$

where $\mathbf{I}$ is the identity matrix.

$$-\omega^2 \varepsilon_0 \mathbf{I}\mathbf{E}_z - \frac{\omega^2 \varepsilon_0 \omega_p^2}{-\omega^2 \mathbf{I} + j\omega \mathbf{v}_c} \mathbf{E}_z = \mathbf{A}\mathbf{E}_z \tag{5}$$

Substitute $\mathbf{\omega_s} = \mathbf{\omega_p^2}$ into (5), and after some algebraic manipulations we have

$$\omega^4 \varepsilon_0 \mathbf{\omega_s}^{-1} \mathbf{E}_z - j\omega^3 \varepsilon_0 \mathbf{V}_c \mathbf{\omega_s}^{-1} \mathbf{E}_z - \omega^2 \varepsilon_0 \mathbf{I}\mathbf{E}_z =$$
$$-\omega^2 \mathbf{\omega_s}^{-1} \mathbf{A}\mathbf{E}_z + j\omega \mathbf{V}_c \, \mathbf{\omega_s}^{-1} \mathbf{A}\mathbf{E}_z \tag{6}$$

$$-j\omega^3 \varepsilon_0 \mathbf{V}_c \mathbf{\omega_s}^{-1} \mathbf{E}_z - \omega^2 \varepsilon_0 \mathbf{I}\mathbf{E}_z + \omega^2 \mathbf{\omega_s}^{-1} \mathbf{A}\mathbf{E}_z$$
$$-j\omega \mathbf{V}_c \, \mathbf{\omega_s}^{-1} \mathbf{A}\mathbf{E}_z = -\omega^4 \varepsilon_0 \mathbf{\omega_s}^{-1} \mathbf{E}_z \tag{7}$$

$$-j\omega^3 \mathbf{V}_c \mathbf{\omega_s}^{-1} \mathbf{E}_z - \omega^2\, \mathbf{I}\,\mathbf{E}_z + \omega^2 \mathbf{\omega_s}^{-1} \frac{\mathbf{A}}{\varepsilon_0} \mathbf{E}_z -$$
$$j\omega \mathbf{V}_c \, \mathbf{\omega_s}^{-1} \frac{\mathbf{A}}{\varepsilon_0} \mathbf{E}_z = -\omega^4 \mathbf{\omega_s}^{-1} \mathbf{E}_z \tag{8}$$

$$j\omega^2 \mathbf{\omega}_s \mathbf{V}_c \mathbf{\omega_s}^{-1} \mathbf{E}_z + \omega \mathbf{\omega}_s \mathbf{E}_z - \omega \frac{\mathbf{A}}{\varepsilon_0} \mathbf{E}_z +$$
$$j\mathbf{\omega}_s \mathbf{V}_c \, \mathbf{\omega_s}^{-1} \frac{\mathbf{A}}{\varepsilon_0} \mathbf{E}_z = \omega^3 \mathbf{E}_z \tag{9}$$

Substituting $\mathbf{B} = j\mathbf{\omega_s}\mathbf{V}_c\mathbf{\omega_s^{-1}}$, $\mathbf{C} = \mathbf{\omega_s} - \dfrac{\mathbf{A}}{\varepsilon_0}$, and $\mathbf{D} = j\mathbf{\omega_s} \mathbf{V}_c \, \mathbf{\omega_s}^{-1} \dfrac{\mathbf{A}}{\varepsilon_0}$ into (9) yields

$$\omega^2 \mathbf{B}\mathbf{E}_z + \omega\mathbf{C}\mathbf{E}_z + \mathbf{D}\mathbf{E}_z = \omega^3 \mathbf{E}_z \tag{10}$$

We can reform (10) into eigenvalue equation

$$\mathbf{H}\mathbf{Z} = \omega\mathbf{Z} \tag{11}$$

where
$$\mathbf{H} = \begin{bmatrix} \mathbf{B} & \mathbf{C} & \mathbf{D} \\ \mathbf{I} & \mathbf{0} & \mathbf{0} \\ \mathbf{0} & \mathbf{I} & \mathbf{0} \end{bmatrix} \quad \text{and} \quad \mathbf{Z} = \begin{bmatrix} \omega^2 \mathbf{E}_z \\ \omega\,\mathbf{E}_z \\ \mathbf{E}_z \end{bmatrix} \tag{12}$$

The quantity ω is the eigenvalue of matrix $\mathbf{H}$, from which we can calculate the normalized eigenfrequencies to be $\omega a/2\pi c$, where a is periodic length and c is the speed of light in free space.

3. Numerical Results

The analysis model is a 2D EBG structure composed of Drude-type dispersive periodic cylinders with square lattice shown in Fig. 1(b). The unit cell contains only one cylinder with radius r , $r/a = 0.2$, $a =1$ mm, and $\Delta x = \Delta y = 0.025$ mm . For the FDFD method, the Arnoldi algorithm [8] is used to compute the eigenvalues of the characteristic matrix. In the FDTD calculation, the recursive-convolution (RC) approach is used to model the Drude dispersive materials [5].

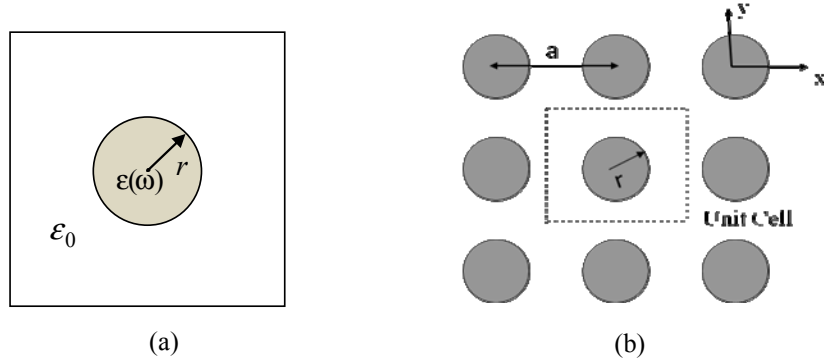(a)   (b)

Fig. 1: (a) unit cell and its contents.   (b) periodic 2D EBG cylinders in square lattice.

First, the band structure is calculated for different values of ω_p , while the value of V_c is set to $5 \cdot 10^{13}$ in all parts of calculation, and the results of FDFD and FDTD are compared. Next, variation of the normalized frequency with respect change in Drude-pole frequency ω_p is discussed using the FDFD method. Finally the electric field distribution of first four eigenmodes is computed using the FDFD method.

Fig. 2(a) shows the band structure computation for $V_c = 5 \cdot 10^{13}$ and $\omega_p = 8 \cdot 10^{14}$. In this calculation, the relative permittivity approaches to a very high value, which causes to create band gap for low frequencies. Both FDFD and FDTD methods have very good agreement except for Γ and M points , because the modes are degenerate. Fig.2(b) shows the band structure calculation for $V_c = 5 \cdot 10^{13}$ and $\omega_p = 8 \cdot 10^{12}$, for which we have low imaginary part of the relative permittivity. In this calculation there is no band gap and most of the mode values overlap each other or there are many degenerate modes, where the FDTD method has irregularities in its calculation due to the degenerate modes because they appear at the same frequency. However, the FDFD method has calculated all the eigenfrequencies because it uses the eigenvalues and can compute all the eigenfrequencies.

(a)   (b)
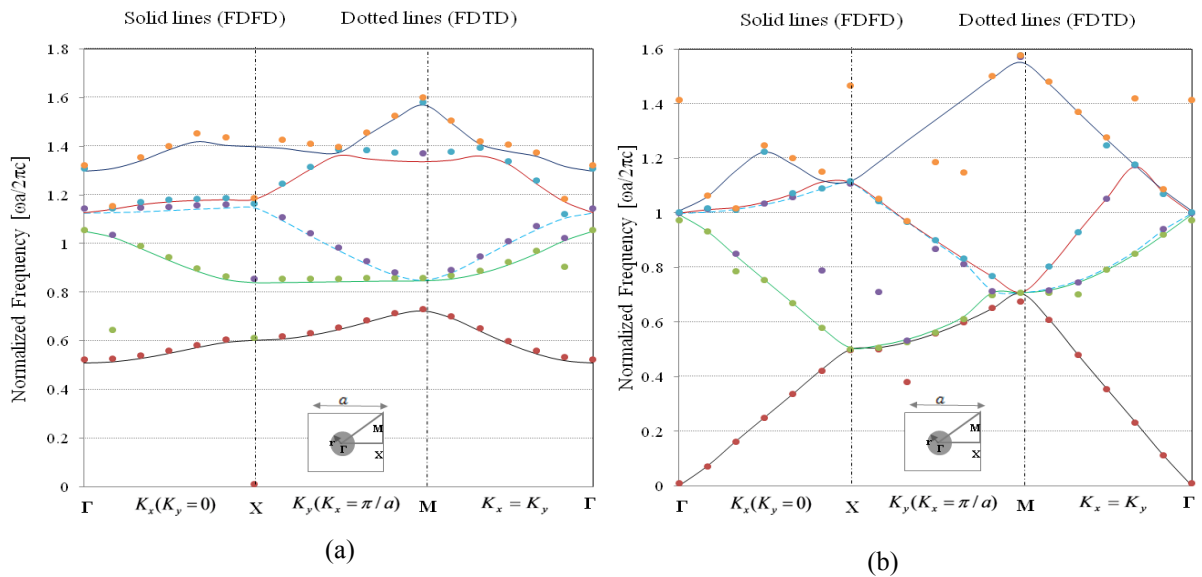
Fig. 2: Band structure calculation using FDFD and FDTD methods. Parts (a) and (b) illustrate the comparison of FDFD and FDTD methods for large and low values of the imaginary part of Drude relative permittivity respectively.

Fig. 2 illustrates that approaching the imaginary part of the Drude relative permittivity to a very large value causes to create band gap for low frequencies, and the band structure seems similar to the that when EBG is composed of perfect electric conductor(PEC). This fact is also seen in electric field distribution of eigenmodes as seen in Fig. 3.
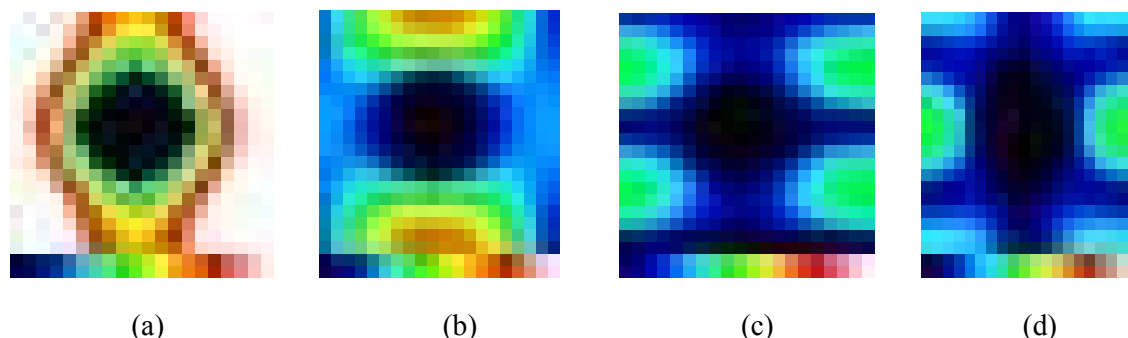

| (a) | (b) | (c) | (d) |

Fig. 3: Electric field distribution of the lowest four eigenmodes for $k_x = 2\pi/3a$ and $k_y = 0$ point of irreducible Brillouin zone computed by the FDFD algorithm. The parts from (a) to (d) show the electric field distribution from first to fourth eigenmodes respectively.

Fig. 3 shows the electric field distribution of the lowest four eigenmodes in unit cell for $V_c = 5 \cdot 10^{13}$ and $\omega_p = 8 \cdot 10^{14}$ using the FDFD algorithm. The fields are normalized and their intensity can be compared with the colour bar placed at the bottom of each part of the figure, where the field intensity increases gradually from left to right in the colour bar. In the circular area of each part of field distribution, the electric field is very weak because in this area the Drude-type EBG cylinder is place that has very large imaginary part of the relative permittivity in this calculation. This case approaches to PEC case, when PEC cylinder is placed in the unit cell. This fact is also seen in Fig. 2 where the Drude-type EBG has band gap for lower frequencies. The calculation of the electric field distribution further confirm the validity and accuracy of the FDFD algorithm for electromagnetic wave behaviour in the Drude-type EBG structures.

5. Conclusion

In this paper, a new FDFD algorithm is used to calculate the band structure and electric field distribution of eigenmodes for 2D TM$_z$ of the EBG structure composed of Drude-type dispersive media. This algorithm successfully calculates the eigenfrequencies of the degenerate modes, as seen at M point of irreducible Brillouin zone, and compute the electric field distribution of each eigenmode distinctly. It relies only on linear algebra and uses the eigenvalue equation; thus it is capable to calculate the band structure and electric field distribution of each eigenmode efficiently and accurately.

References

[1] K. Yasumoto, *Electromagnetic Theory and Application for Photonic Crystal*s, CRC press, Boca Raton, FL, 2006.
[2] K. Sakoda, *Optical Properties of Photonic Crystals*, 2nd Ed., Springer-Verlag, Berlin Heidelberg, 2005
[3] A. Taflove and S. C. Hagness, *Computational Electrodynamics: The Finite-Difference Time -Domain Method*, 3rd Ed., Artech House, Norwood, MA, 2005.
[4] T. Uno, *Finite-Difference Time – Domain Method for Electromagnetic Field and Antenna Analysis*, Corona Publishing Co. LTD. 1998 (in Japanese).
[5] D. F. Kelley and R. J. Luebbers, "Piecewise Linear Recursive Convolution for Dispersive Media Using FDTD," *IEEE Trans. on Antenna and Propagat*., vol. 44, no. 6, June 1996.
[6] Y. C. Chiang, Y. P. Chiou, and H. C. Chang, "Finite-Difference Frequency-Domain Analysis of 2-D Photonic Crystals With Curved Dielectric interfaces," *Lightwave Tech*., vol. 26, no. 8, Apr. 2008.
[7] A. G. Hanif, T. Uno, and T. Arima, "Finite-Difference Frequency-Domain Algorithm For Band Diagram Calculation of 2-D Photonic Crystals Composed of Debye Type Dispersive Materials"*IEEE Antenna and Wireless Propagat. Lett.* Vol. 11, 41-44, 2012
[8] http://www.caam.rice.edu/software/ARPACK/